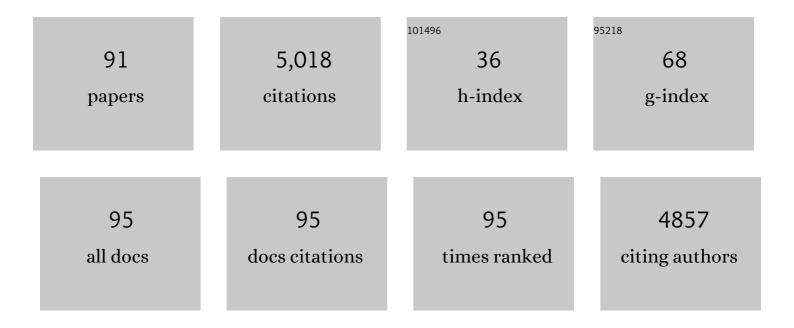
List of Publications by Year in descending order

Source: https://exaly.com/author-pdf/3524685/publications.pdf Version: 2024-02-01



MATS SANDOREN

#	Article	IF	CITATIONS
1	Fungal Cellulases. Chemical Reviews, 2015, 115, 1308-1448.	23.0	673
2	The Putative Endoglucanase PcGH61D from Phanerochaete chrysosporium Is a Metal-Dependent Oxidative Enzyme that Cleaves Cellulose. PLoS ONE, 2011, 6, e27807.	1.1	226
3	Quantum mechanical calculations suggest that lytic polysaccharide monooxygenases use a copper-oxyl, oxygen-rebound mechanism. Proceedings of the National Academy of Sciences of the United States of America, 2014, 111, 149-154.	3.3	210
4	The First Structure of a Glycoside Hydrolase Family 61 Member, Cel61B from Hypocrea jecorina, at 1.6ÂÃ Resolution. Journal of Molecular Biology, 2008, 383, 144-154.	2.0	197
5	The Mechanism of Cellulose Hydrolysis by a Two-Step, Retaining Cellobiohydrolase Elucidated by Structural and Transition Path Sampling Studies. Journal of the American Chemical Society, 2014, 136, 321-329.	6.6	164
6	Crystal Structure and Computational Characterization of the Lytic Polysaccharide Monooxygenase GH61D from the Basidiomycota Fungus Phanerochaete chrysosporium. Journal of Biological Chemistry, 2013, 288, 12828-12839.	1.6	158
7	Structural and Functional Characterization of a Lytic Polysaccharide Monooxygenase with Broad Substrate Specificity. Journal of Biological Chemistry, 2015, 290, 22955-22969.	1.6	157
8	Glycosylated linkers in multimodular lignocellulose-degrading enzymes dynamically bind to cellulose. Proceedings of the National Academy of Sciences of the United States of America, 2013, 110, 14646-14651.	3.3	149
9	Oxygen Activation by Cu LPMOs in Recalcitrant Carbohydrate Polysaccharide Conversion to Monomer Sugars. Chemical Reviews, 2018, 118, 2593-2635.	23.0	143
10	Interactions of a fungal lytic polysaccharide monooxygenase with β-glucan substrates and cellobiose dehydrogenase. Proceedings of the National Academy of Sciences of the United States of America, 2016, 113, 5922-5927.	3.3	126
11	The X-ray crystal structure of the Trichoderma reesei family 12 endoglucanase 3, Cel12A, at 1.9 Ã resolution1 1Edited by A. R. Fersht. Journal of Molecular Biology, 2001, 308, 295-310.	2.0	121
12	Structural and biochemical studies of CH family 12 cellulases: improved thermal stability, and ligand complexes. Progress in Biophysics and Molecular Biology, 2005, 89, 246-291.	1.4	113
13	Improved bio-energy yields via sequential ethanol fermentation and biogas digestion of steam exploded oat straw. Bioresource Technology, 2011, 102, 4449-4455.	4.8	112
14	Biofuel production from straw hydrolysates: current achievements and perspectives. Applied Microbiology and Biotechnology, 2019, 103, 5105-5116.	1.7	112
15	Structural and Electronic Snapshots during the Transition from a Cu(II) to Cu(I) Metal Center of a Lytic Polysaccharide Monooxygenase by X-ray Photoreduction. Journal of Biological Chemistry, 2014, 289, 18782-18792.	1.6	99
16	Towards a molecular-level theory of carbohydrate processivity in glycoside hydrolases. Current Opinion in Biotechnology, 2014, 27, 96-106.	3.3	89
17	Recombinant expression of thermostable processive MtEG5 endoglucanase and its synergism with MtLPMO from Myceliophthora thermophila during the hydrolysis of lignocellulosic substrates. Biotechnology for Biofuels, 2017, 10, 126.	6.2	76
18	Structural, Biochemical, and Computational Characterization of the Glycoside Hydrolase Family 7 Cellobiohydrolase of the Tree-killing Fungus Heterobasidion irregulare*. Journal of Biological Chemistry, 2013, 288, 5861-5872.	1.6	70

#	Article	IF	CITATIONS
19	Biochemical profiling, prediction of total lipid content and fatty acid profile in oleaginous yeasts by FTIR spectroscopy. Biotechnology for Biofuels, 2019, 12, 140.	6.2	70
20	Comparison of family 12 glycoside hydrolases and recruited substitutions important for thermal stability. Protein Science, 2003, 12, 848-860.	3.1	69
21	Biochemical Characterization and Crystal Structures of a Fungal Family 3 β-Glucosidase, Cel3A from Hypocrea jecorina. Journal of Biological Chemistry, 2014, 289, 31624-31637.	1.6	68
22	Structural and functional studies of a Fusarium oxysporum cutinase with polyethylene terephthalate modification potential. Biochimica Et Biophysica Acta - General Subjects, 2015, 1850, 2308-2317.	1.1	68
23	X-ray Structures of the Maltose–Maltodextrin-binding Protein of the Thermoacidophilic Bacterium Alicyclobacillus acidocaldarius Provide Insight into Acid Stability of Proteins. Journal of Molecular Biology, 2004, 335, 261-274.	2.0	66
24	High-resolution structure of a lytic polysaccharide monooxygenase from Hypocrea jecorina reveals a predicted linker as an integral part of the catalytic domain. Journal of Biological Chemistry, 2017, 292, 19099-19109.	1.6	61
25	Proteome analysis of xylose metabolism in Rhodotorula toruloides during lipid production. Biotechnology for Biofuels, 2019, 12, 137.	6.2	61
26	Comparison of three seemingly similar lytic polysaccharide monooxygenases from Neurospora crassa suggests different roles in plant biomass degradation. Journal of Biological Chemistry, 2019, 294, 15068-15081.	1.6	59
27	Lipid production from hemicellulose with <i>Lipomyces starkeyi</i> in a pH regulated fedâ€batch cultivation. Yeast, 2016, 33, 451-462.	0.8	56
28	A systems analysis of biodiesel production from wheat straw using oleaginous yeast: process design, mass and energy balances. Biotechnology for Biofuels, 2016, 9, 229.	6.2	55
29	Genomeâ€scale model of <i>Rhodotorula toruloides</i> metabolism. Biotechnology and Bioengineering, 2019, 116, 3396-3408.	1.7	55
30	Manganese and iron deficiency in Southern Ocean Phaeocystis antarctica populations revealed through taxon-specific protein indicators. Nature Communications, 2019, 10, 3582.	5.8	53
31	Disruption of the Eng18B ENGase Gene in the Fungal Biocontrol Agent Trichoderma atroviride Affects Growth, Conidiation and Antagonistic Ability. PLoS ONE, 2012, 7, e36152.	1.1	52
32	Improving the thermal stability of cellobiohydrolase Cel7A from Hypocrea jecorina by directed evolution. Journal of Biological Chemistry, 2017, 292, 17418-17430.	1.6	52
33	Effect of lignin fractions isolated from different biomass sources on cellulose oxidation by fungal lytic polysaccharide monooxygenases. Biotechnology for Biofuels, 2018, 11, 296.	6.2	52
34	Bioethanol and lipid production from the enzymatic hydrolysate of wheat straw after furfural extraction. Applied Microbiology and Biotechnology, 2018, 102, 6269-6277.	1.7	46
35	Three-Dimensional Structure of an Intact Glycoside Hydrolase Family 15 Glucoamylase from Hypocrea jecorina. Biochemistry, 2008, 47, 5746-5754.	1.2	45
36	Oleaginous yeast as a component in fish feed. Scientific Reports, 2018, 8, 15945.	1.6	45

#	Article	lF	CITATIONS
37	Microbial lipid production from crude glycerol and hemicellulosic hydrolysate with oleaginous yeasts. Biotechnology for Biofuels, 2021, 14, 65.	6.2	41
38	The dissociation mechanism of processive cellulases. Proceedings of the National Academy of Sciences of the United States of America, 2019, 116, 23061-23067.	3.3	40
39	TheHumicola griseaCel12A enzyme structure at 1.2 â,,« resolution and the impact of its free cysteine residues on thermal stability. Protein Science, 2003, 12, 2782-2793.	3.1	37
40	Sequencing, biochemical characterization, crystal structure and molecular dynamics of cellobiohydrolase Cel7A from <i>Geotrichum candidum</i> 3C. FEBS Journal, 2015, 282, 4515-4537.	2.2	37
41	Correlation of structure, function and protein dynamics in GH7 cellobiohydrolases from Trichoderma atroviride, T. reesei and T. harzianum. Biotechnology for Biofuels, 2018, 11, 5.	6.2	37
42	Oleaginous yeasts respond differently to carbon sources present in lignocellulose hydrolysate. Biotechnology for Biofuels, 2021, 14, 124.	6.2	37
43	Structural and molecular dynamics studies of a C1â€oxidizing lytic polysaccharide monooxygenase from <i>Heterobasidion irregulare</i> reveal amino acids important for substrate recognition. FEBS Journal, 2018, 285, 2225-2242.	2.2	35
44	The Structure of a Bacterial Cellobiohydrolase: The Catalytic Core of the Thermobifida fusca Family GH6 Cellobiohydrolase Cel6B. Journal of Molecular Biology, 2013, 425, 622-635.	2.0	34
45	Crystal Complex Structures Reveal How Substrate is Bound in the â~'4 to the +2 Binding Sites of Humicola grisea Cel12A. Journal of Molecular Biology, 2004, 342, 1505-1517.	2.0	32
46	Loop Motions Important to Product Expulsion in the Thermobifida fusca Glycoside Hydrolase Family 6 Cellobiohydrolase from Structural and Computational Studies. Journal of Biological Chemistry, 2013, 288, 33107-33117.	1.6	31
47	Biochemical studies of two lytic polysaccharide monooxygenases from the white-rot fungus Heterobasidion irregulare and their roles in lignocellulose degradation. PLoS ONE, 2017, 12, e0189479.	1.1	31
48	Xâ€ray crystal structures of <i>Phanerochaete chrysosporium</i> Laminarinase 16A in complex with products from lichenin and laminarin hydrolysis. FEBS Journal, 2009, 276, 3858-3869.	2.2	30
49	Microplate-Based Detection of Lytic Polysaccharide Monooxygenase Activity by Fluorescence-Labeling of Insoluble Oxidized Products. Biomacromolecules, 2017, 18, 610-616.	2.6	30
50	Evolution and functional characterization of pectate lyase PEL12, a member of a highly expanded Clonostachys rosea polysaccharide lyase 1 family. BMC Microbiology, 2018, 18, 178.	1.3	29
51	Structural and functional studies of the glycoside hydrolase family 3 β-glucosidase Cel3A from the moderately thermophilic fungus <i>Rasamsonia emersonii</i> . Acta Crystallographica Section D: Structural Biology, 2016, 72, 860-870.	1.1	28
52	Greenhouse gas performance of biochemical biodiesel production from straw: soil organic carbon changes and time-dependent climate impact. Biotechnology for Biofuels, 2017, 10, 217.	6.2	28
53	Expression, crystal structure and cellulase activity of the thermostable cellobiohydrolase Cel7A from the fungus <i>Humicola grisea</i> var. <i>thermoidea</i> . Acta Crystallographica Section D: Biological Crystallography, 2014, 70, 2356-2366.	2.5	26
54	Functionalized silk assembled from a recombinant spider silk fusion protein (Zâ€4RepCT) produced in the methylotrophic yeast <i>Pichia pastoris</i> . Biotechnology Journal, 2016, 11, 687-699.	1.8	26

#	Article	IF	CITATIONS
55	High Resolution Crystal Structure of the Endo-N-Acetyl-β-D-Glucosaminidase Responsible for the Deglycosylation of Hypocrea jecorina Cellulases. PLoS ONE, 2012, 7, e40854.	1.1	25
56	Structural insights into the inhibition of cellobiohydrolase Cel7A by xyloâ€oligosaccharides. FEBS Journal, 2015, 282, 2167-2177.	2.2	25
57	Mutations That Affect Ligand Binding to the Escherichia coli Aspartate Receptor. Journal of Biological Chemistry, 2001, 276, 2808-2815.	1.6	23
58	Synthesis of Cyclic β-Glucan Using Laminarinase 16A Glycosynthase Mutant from the Basidiomycete Phanerochaete chrysosporium. Journal of the American Chemical Society, 2010, 132, 1724-1730.	6.6	22
59	Identification ofArabidopsis thaliana sequences responsive to low temperature and abscisic acid by T-DNA tagging andin-vivo gene fusion. Plant Molecular Biology Reporter, 1995, 13, 243-254.	1.0	18
60	Airtight storage of moist wheat grain improves bioethanol yields. Biotechnology for Biofuels, 2009, 2, 16.	6.2	17
61	Identification of proteins that specifically recognize and bind protofibrillar aggregates of amyloid-β. Scientific Reports, 2017, 7, 5949.	1.6	17
62	Genetic variation of biomass recalcitrance in a natural Salix viminalis (L.) population. Biotechnology for Biofuels, 2019, 12, 135.	6.2	17
63	Identification, Quantification and Kinetic Study of Carotenoids and Lipids in Rhodotorula toruloides CBS 14 Cultivated on Wheat Straw Hydrolysate. Fermentation, 2022, 8, 300.	1.4	16
64	Rational design, synthesis, evaluation and enzyme – substrate structures of improved fluorogenic substrates for familyÂ6 glycoside hydrolases. FEBS Journal, 2013, 280, 184-198.	2.2	14
65	Rational Design of Spider Silk Materials Genetically Fused with an Enzyme. Advanced Functional Materials, 2015, 25, 5343-5352.	7.8	14
66	Hydrolysis and Transglycosylation Transition States of Glycoside Hydrolase Family 3 β-Glucosidases Differ in Charge and Puckering Conformation. Journal of Physical Chemistry B, 2018, 122, 9452-9459.	1.2	14
67	X-ray crystallographic native sulfur SAD structure determination of laminarinase Lam16A fromPhanerochaete chrysosporium. Acta Crystallographica Section D: Biological Crystallography, 2006, 62, 1422-1429.	2.5	13
68	The Crystal Structure of the Core Domain of a Cellulose Induced Protein (Cip1) from Hypocrea jecorina, at 1.5 Ã Resolution. PLoS ONE, 2013, 8, e70562.	1.1	13
69	Machine learning reveals sequence-function relationships in family 7 glycoside hydrolases. Journal of Biological Chemistry, 2021, 297, 100931.	1.6	13
70	The role of catalytic residue p <i>K</i> _a on the hydrolysis/transglycosylation partition in family 3 β-glucosidases. Organic and Biomolecular Chemistry, 2018, 16, 316-324.	1.5	12
71	FT-NIR: a tool for rapid intracellular lipid quantification in oleaginous yeasts. Biotechnology for Biofuels, 2019, 12, 169.	6.2	12
72	Biomass Recalcitrance in Willow Under Two Biological Conversion Paradigms: Enzymatic Hydrolysis and Anaerobic Digestion. Bioenergy Research, 2020, 13, 260-270.	2.2	10

#	Article	IF	CITATIONS
73	Backbone and side-chain 1H, 13C, and 15N chemical shift assignments for the apo-form of the lytic polysaccharide monooxygenase NcLPMO9C. Biomolecular NMR Assignments, 2016, 10, 277-280.	0.4	8
74	A fineâ€ŧuned composition of protein nanofibrils yields an upgraded functionality of displayed antibody binding domains. Biotechnology Journal, 2017, 12, 1600672.	1.8	8
75	Assembly and Analysis of the Genome Sequence of the Yeast Brettanomyces naardenensis CBS 7540. Microorganisms, 2019, 7, 489.	1.6	8
76	Protofibrillar and Fibrillar Amyloid-β Binding Proteins in Cerebrospinal Fluid. Journal of Alzheimer's Disease, 2018, 66, 1053-1064.	1.2	7
77	Side-by-side biochemical comparison of two lytic polysaccharide monooxygenases from the white-rot fungus Heterobasidion irregulare on their activity against crystalline cellulose and glucomannan. PLoS ONE, 2018, 13, e0203430.	1.1	7
78	Production of Ready-To-Use Functionalized Sup35 Nanofibrils Secreted by <i>Komagataella pastoris</i> . ACS Nano, 2018, 12, 9363-9371.	7.3	7
79	Structural studies of a glycoside hydrolase family 3 β-glucosidase from the model fungus <i>Neurospora crassa</i> . Acta Crystallographica Section F, Structural Biology Communications, 2018, 74, 787-796.	0.4	7
80	Comparison of Glycoside Hydrolase family 3 β-xylosidases from basidiomycetes and ascomycetes reveals evolutionarily distinct xylan degradation systems. Journal of Biological Chemistry, 2022, , 101670.	1.6	7
81	α-Galactobiosyl units: thermodynamics and kinetics of their formation by transglycosylations catalysed by the GH36 α-galactosidase from Thermotoga maritima. Carbohydrate Research, 2015, 401, 115-121.	1.1	6
82	Enantioselective Binding of Propranolol and Analogues Thereof to Cellobiohydrolase Cel7A. Chemistry - A European Journal, 2018, 24, 17975-17985.	1.7	5
83	Kinetic and molecular dynamics study of inhibition and transglycosylation in Hypocrea jecorina family 3 β-glucosidases. Journal of Biological Chemistry, 2019, 294, 3169-3180.	1.6	5
84	Inhibition of cytosine methylation allows efficient cloning of T-DNA tagged plant DNA ofArabidopsis thaliana by plasmid rescue. In Vitro Cellular and Developmental Biology - Plant, 1994, 30, 204-209.	0.9	4
85	The method of integrated kinetics and its applicability to the exo-glycosidase-catalyzed hydrolysis of p-nitrophenyl glycosides. Carbohydrate Research, 2015, 412, 43-49.	1.1	4
86	Coupled chemistry kinetics demonstrate the utility of functionalized Sup35 amyloid nanofibrils in biocatalytic cascades. Journal of Biological Chemistry, 2019, 294, 14966-14977.	1.6	4
87	Enhanced detection of ATTR amyloid using a nanofibril-based assay. Amyloid: the International Journal of Experimental and Clinical Investigation: the Official Journal of the International Society of Amyloidosis, 2021, 28, 158-167.	1.4	4
88	Temperatureâ€dependent changes in the microbial storage flora of birch and spruce sawdust. Biotechnology and Applied Biochemistry, 2014, 61, 58-64.	1.4	3
89	Glucomannan and beta-glucan degradation by Mytilus edulis Cel45A: Crystal structure and activity comparison with GH45 subfamily A, B and C. Carbohydrate Polymers, 2022, 277, 118771.	5.1	3
90	The kinetics of TEM1 antibiotic degrading enzymes that are displayed on Ure2 protein nanofibrils in a flow reactor. PLoS ONE, 2018, 13, e0196250.	1.1	2

#	Article	IF	CITATIONS
91	The Dissociation Mechanism of the Processive Cellulase TrCel7A. Biophysical Journal, 2020, 118, 531a-532a.	0.2	1